Synthesis, Redox Chemistry, and Mixed-Valence Phenomena of Cyanide-Bridged Dinuclear Organometallic Complexes

Nianyong Zhu and Heinrich Vahrenkamp*

Institut für Anorganische und Analytische Chemie der Universität Freiburg,
Albertstrasse 21, D-79104 Freiburg, Germany

Received April 28, 1997

Keywords: Organometallic complexes / Cyanide bridges / Structure elucidation / Isomerizations / Oxidation / Mixed valent compounds

21 new organometallic complexes of the type M−CN−M′ containing the building blocks M, M′ = $(CO)_5Cr$, $(CO)_5Mo$, $(CO)_5W$, $Cp(CO)_2Mn$, $Cp(CO)_2Fe$, $Cp(CO)(CN)Fe$, $Cp(dppe)Fe$, $Cp(PPh_3)_2Ru$, $Cp(PPh_3)Ni$, and $(PPh_3)_2Ag$ were obtained from the reagents M−CN and M−X (X = leaving group). Among them are five pairs of linkage isomers M−CN−M′/M−NC−M′. Structure determinations of $(CO)_5Cr-CN-M'$ with M′ = Fe(dppe)Cp, $Ni(PPh_3)Cp$, $Ag(PPh_3)_2$ and of $(CO)_5Cr-NC-Fe(dppe)Cp$ have proved their identity and the linkage isomerism. Systematic variations of the ν(CN) and ν(CO) IR bands allow an assessment of the relative electron pair acceptor strengths of the building blocks M and M′ and a reliable identification of the individual linkage isomers. All dinuclear complexes are redox-active, showing at least one reversible oxidation. The redox potentials are characteristically dependent upon the nature of the building blocks M and M′ and upon the orientation of the cyanide link (CN vs. NC). 6 oxidized complexes of the type $[M-CN-Fe(dppe)Cp]^+$ were prepared chemically and isolated as PF_6 or BF_4 salts. The molecular structure of $[(CO)_5Cr-CN-Fe(dppe)Cp]BF_4$ is not significantly different from those of the corresponding neutral Cr−CN−Fe or Cr−NC−Fe complexes. Upon oxidation the ν(CN) band of the complexes shifts to lower wavenumbers and becomes much more intense. The oxidized complexes show the paramagnetism due to one unpaired electron. They give rise to very intense metal-to-metal charge-transfer bands in the near infrared region whose postion was found to be characteristically dependent on solvent polarity for $[(CO)_5Cr-CN-Fe(dppe)Cp]BF_4$. A semiquantitative treatment of the optical and electrochemical measurements shows that the electron delocalization and metal−metal interaction in the oxidized dinuclear complexes is significant and that they belong to the class-II mixed-valence systems.

The colour of Prussian Blue, the oldest mixed-valence compound, results from a metal-to-metal charge transfer (MMCT) from *C*-bound Fe^{II} to *N*-bound Fe^{III} via bridging cyanide ions. It visualizes ligand-mediated metal-metal interactions in a solid state material which give rise to colour and electrical conductivity and which in recent years have been exploited for the design of new magnetic materials based on heterometallic cyanides.[1][2][3]

In order to reduce the complexity of the electronic situation and at the same time increase the variability of a chemical approach, 2- and 1-dimensional variants of the polymeric cyanide-bridged compounds have been prepared.[4][5][6][7][8][9] They were again attractive because of their magnetic[6][7] and electrical properties.[8][9]

When the dimensionality of the systems is further reduced to the molecular level, materials properties of the oligometallic cyanide-bridged complexes can no longer be expected. Instead the electronic interactions between two metal centers can be modified and investigated to a much greater degree. This has been demonstrated successfully by, among others, the research groups of Connelly,[10][11] Fehlhammer,[12] Shriver,[13] Scandola,[14][15] Haim,[16] Vogler,[17] and Denning,[18] based on the well-known fact that cyanide is a good donor at both its C and N atoms.[19] Quite recently another incentive to study dimetallic metallocyanides has emerged from the observation that cyanide-poisoning of the enzyme cytochrome c oxidase may be related to cyanide bridging between iron and copper centers, which has led to the investigation of some copper-containing model compounds.[20][21]

We became attracted to the chemistry of cyanide ligands during our work on the interconversions of small substrate molecules attached to clusters in a face bridging manner.[22] We then realized that organometallic cyanide complexes are very good synthons because of their Lewis basicity, inertness, and ease of preparation, three properties which to our surprise have been exploited to an unusually low degree so far, which may be related to the general opinion that cyanide complexes are classical coordination compounds. After first preparing some cluster-derived organometallic cyanides[23][24][25] we are now focusing on systems with chain-like arrays of cyanide-linked organometallic units. Our aim is to improve our understanding of organometallic redox chemistry[26] and to find new types of electronic (e.g. magnetic) interactions between distant metal centers.

This paper reports basic results on the synthesis of dinuclear complexes of the type M−CN−M′, on their structures and M−CN−M′/M−NC−M′ linkage isomerism, and on their redox chemistry resulting in species with one unpaired electron. The spectroscopic features accompanying oxidation are discussed in relation to the properties of the cyanide ligand and to the phenomenon of

 © VCH Verlagsgesellschaft mbH, D-69451 Weinheim, 1997 0009−2940/97/0909−1241 $ 17.50+.50/0

mixed valence. Two results of this work have been published as short communications.[27][28] Further papers will deal with oligonuclear systems, with the incorporation of redox-active coligands, and with magnetic interactions in multi-spin systems.

Preparations

All the cyanide-bridged dinuclear compounds described here are organometallic rather than classical complexes. Thereby we hoped to achieve inertness and ease of preparation without sacrificing a productive redox chemistry. The latter requires an appropriate ligand pattern of the organometallic building blocks. For this purpose Connelly et al.[10][11] have used species which are rich in phosphane ligands. We found that cyclopentadienyl ligands serve the same purpose.

The simplest homodinuclear organometallic complexes $[M-CN-M]^-$ for M = $(CO)_5Cr$, $(CO)_5Mo$, $(CO)_5W$, and $(CO)_4Fe$ have been described long ago.[29][30] We contributed the complex with M = $Cp(CO)_2Mn$.[23] The species with M = $Cp(dppe)Fe^+$ was prepared and subjected to one-electron oxidation by Connelly,[11] the one with M = $Cp(PPh_3)_2Ru^+$ by Davies.[31] The list of heterodinuclear complexes is already quite extensive, cf. ref.[10][12][23] and references cited therein. However, not too many of them have been subjected to redox investigations. Optical and magnetic measurements related to the question of electronic interactions are scarce, and to our knowledge prior to our work no pair of linkage isomers M−CN−M′/M−NC−M′ had been isolated among the organometallic compounds.

The new cyanide-bridged complexes were prepared by the conventional procedure of mixing an organometallic cyanide M−CN with a suitable complex M′−X bearing a good leaving group X as a ligand. The complexes M−CN were **a**–**h**, the complexes M′−X were **i**–**p**.

$Na[(CO)_5Cr-CN]$ **a**	$Na[(CO)_5Mo-CN]$ **b**
$Na[(CO)_5W-CN]$ **c**	$Na[Cp(CO)_2Mn-CN]$ **d**
$Cp(CO)_2Fe-CN$ **e**	$Cp(dppe)Fe-CN$ **f**
$K[Cp(CO)Fe(CN)_2]$ **g**	$Cp(PPh_3)_2Ru-CN$ **h**
$(CO)_5Cr-THF$ **i**	$(CO)_5Mo-THF$ **j**
$(CO)_5W-THF$ **k**	$Cp(CO)_2Mn-THF$ **l**
$[Cp(CO)_2Fe-THF]BF_4$ **m**	$Cp(dppe)Fe-Br$ **n**
$Cp(PPh_3)Ni-Cl$ **o**	$(PPh_3)_2AgNO_3$ **p**

Of the 64 possible combinations between these reagents we found 10 in the literature, including the 6 symmetrical ones mentioned above.[11][23][29][30][31] We tried 24 here of which 21 were successful, leading to the dinuclear complexes listed below.

$(CO)_5Cr-CN-FeCp(CO)_2$ **1a**	$(CO)_5Cr-NC-FeCp(CO)_2$ **1b**
$(CO)_5Cr-CN-Fe(dppe)Cp$ **2a**	$(CO)_5Cr-NC-Fe(dppe)Cp$ **2b**
$(CO)_5Cr-CN-Ni(PPh_3)Cp$ **3**	$(CO)_5Cr-CN-Ag(PPh_3)_2$ **4**
$(CO)_5Mo-CN-FeCp(CO)_2$ **5**	$(CO)_5Mo-CN-Fe(dppe)Cp$ **6**
$(CO)_5Mo-CN-Ni(PPh_3)(Cp$ **7**	$(CO)_5W-CN-Fe(dppe)Cp$ **8**
$(CO)_5W-CN-Fe(CO)_2Cp$ **9a**	$(CO)_5W-NC-Fe(CO)_2Cp$ **9b**
$(CO)_5W-CN-Ni(PPh_3)Cp$ **10**	$[Cp(CO)_2Fe-CN-Fe(CO)_2Cp]BF_4$ **11**
$Cp(CO)_2Fe-CN-Mn(CO)_2Cp$ **12a**	$Cp(CO)_2Fe-NC-Mn(CO)_2Cp$ **12b**
$[Cp(CO)_2Fe-CN-Fe(dppe)Cp]PF_6$ **13**	$Cp(CO)(CN)Fe-CN-Fe(dppe)Cp$ **14**
$Cp(dppe)Fe-CN-Mn(CO)_2Cp$ **15a**	$Cp(dppe)Fe-NC-Mn(CO)_2Cp$ **15b**
$[Cp(PPh_3)_2Ru-CN-Fe(dppe)Cp]PF_6$ **16**	

The unsuccessful attempts were aimed at dinuclear complexes with $(CO)_5Mo-NC$ units which seem to be too labile. To our surprise the cation $[Cp(dppe)Fe-CN-Fe(CO)_2Cp]^+$ proved unstable too. Among the new complexes is one symmetrical case, **11**. Five pairs of linkage isomers M−CN−M′/M−NC−M′ (**1**, **2**, **9**, **12**, **15**) were obtained. We could not observe any physical changes of the individual components of those pairs when they were heated as solids or in solution before decomposition set in. Thus they seem to be inert towards isomerisation.

Complexes **11**, **12a**, and **12b** complete a series of isoelectronic complexes which includes the known complex $PPN[Cp(CO)_2Mn-CN-Mn(CO)_2Cp]$.[23] The highly symmetrical structure of the latter was determined,[23] and it is to be assumed that the three other complexes resemble it structurally and electronically although they show characteristically different colours and spectra.

Structures of Neutral Complexes

Four complexes were subjected to structure determinations. In order to simplify the discussion they were all chosen to contain $(CO)_5Cr$ as one of the organometallic building blocks. In order to complement the known structures of M−CN−M′ complexes with M/M′ units from the chromium and manganese triads, their M′ units were chosen to contain Fe, Ni, and Ag.

Both linkage isomers of the pair **2a**/**2b** gave suitable crystals. It turned out that they are isomorphous and that their structures can be represented by a single drawing, Figure 1. For this reason it was ascertained that the colours of **2a** (red) and **2b** (yellow) had not changed after data collection and that the IR spectra taken from the crystals after data collection were still those of the different individuals. **2a** and **2b** comprise the first proven case of M−CN−M′/M−NC−M′ linkage isomerism for organometallic complexes. There are a few such cases in classical coordination chemistry,[12] the first crystallographically proven pair being the $(NH_3)_5Co(\mu\text{-}CN)Co(CN)_5$ complexes,[32][33] while linkage isomerism for terminal cyanide is still a matter of dispute.[12]

The important structural features of **2a** and **2b** are compared in Table 1. The $(CO)_5Cr$ and Fe(dppe)Cp moieties have chromium and iron in the typical octahedral or piano stool geometries, respectively. The differences in all bond

Figure 1. Molecular structure of **2a** (with the Cr–C–N–Fe arrangement) and **2b** (with the Cr–N–C–Fe arrangement); selected bond lengths and angles see Table 1

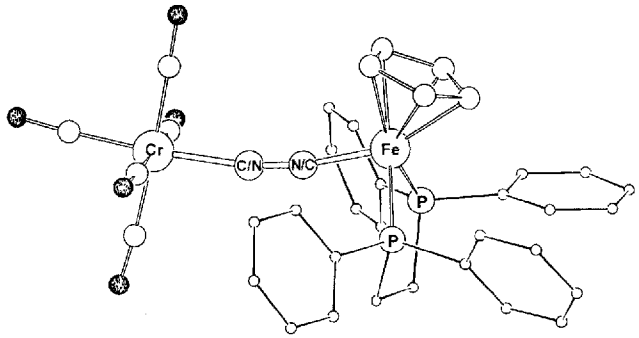

Table 1. Pertinent bond lengths [Å] and angles [°] for **2a** and **2b**

Bond length/angle	**2a**	**2b**
Fe–N/Fe–C(CN)	1.935(4)	1.897(4)
Fe–P1	2.200(1)	2.184(1)
Fe–P2	2.204(1)	2.187(1)
Cr–C/Cr–N(CN)	2.064(5)	2.086(3)
Cr–C(CO-*trans*)	1.838(6)	1.844(5)
Cr–C(CO-*cis*,av.)	1.886(7)	1.895(6)
C–N	1.158(7)	1.151(5)
Fe–N–C/Fe–C–N	169.8(4)	174.3(4)
Cr–C–N/Cr–N–C	170.7(4)	165.1(3)

lengths are quite small. Thus Fe–C in **2b** is shorter than Fe–N in **2a**, and likewise Cr–C in **2a** is shorter than Cr–N in **2b**, corresponding to cyanide being a better π-acceptor at its carbon terminus. Accordingly the Fe–P bonds in **2a** are longer than those in **2b** which has the less electron-rich iron atom, but the Cr–C(CO-*trans*) distances do not reflect the more electron-rich nature of chromium in **2b** by a shortening.

The M–C–N–M′ arrangement in both complexes is distinctly nonlinear, more so than in most other M–CN–M′ structures reported so far.[10][11][12][13][14][15] While packing forces are usually invoked to explain the nonlinearity, the difference between **2a** and **2b** in this respect points to an electronic influence. In both cases the M–N–C angle deviates more from 180° than the M–C–N angle. This can be related to the backbonding or "linearizing" capacity of the N and C termini of the cyanide ligand which is consistently larger for carbon.

The central feature of both complexes, the C–N bond length, is identical within the error limit for both structures. Its value, 1.15–1.16 Å, is within the small range of lengths reported for C–N in all cyanide complexes.[12][34][35] Accordingly, it seems to be of a generally low value for bonding discussions. However, the close overall similarity of **2a** and **2b** in all their geometrical details underlines the ability of the bridging cyanide ligand for delocalization and the leveling out of electronic imbalances.

The molecular structures of the Cr–CN–Ni complex **3** (Figure 2) and the Cr–CN–Ag complex **4** (Figure 3) are variations of the principles outlined above. **3** crystallizes with two molecules per asymmetric unit which differ by a 30° rotation of the two organometallic units around the Cr–CN–Ni axis while their other molecular features are nearly identical. The Cr–C(CN) bond in **3** is slightly shorter than in **2a**, the Cr–C(CO-*trans*) bond is slightly longer which may express a slightly better π-acceptor ability of $Cp(PPh_3)Ni–NC$ vs. Cp(dppe)Fe–NC. The C–N bond length is normal again, but the Cr–C–N–Ni arrangement is closer to linearity than in **2a**/**2b**. The ligand arrangement and bond lengths around the nickel atom are close to those in other complexes $Cp(PPh_3)Ni–X$ (X = R[36] or SR[37]).

Figure 2. Molecular structure of **3**[a]

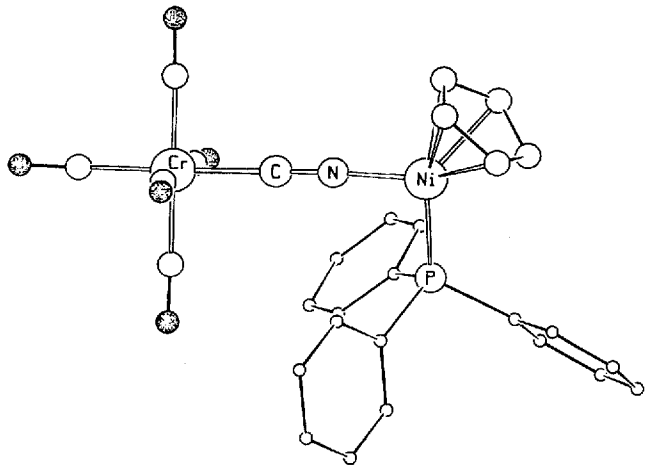

[a]Selected bond lengths [Å] and angles [°] for the two independent molecules in the asymmetric unit: Cr–C1 2.026(4)/2.023(3), Cr–C (CO-*trans*) 1.855(4)/1.852(4), Cr–C (CO-*cis*, av.) 1.886(5)/1.890(5), C1–N1 1.143(4)/1.149(4), Ni–N1 1.852(3)/1.856(3), Ni–P 2.151(1)/2.156(1), Cr–C1–N1 177.1(3)/176.4(3), Ni–N1–C1 177.1(3)/171.5(3).

Figure 3. Molecular structure of **4**[a]

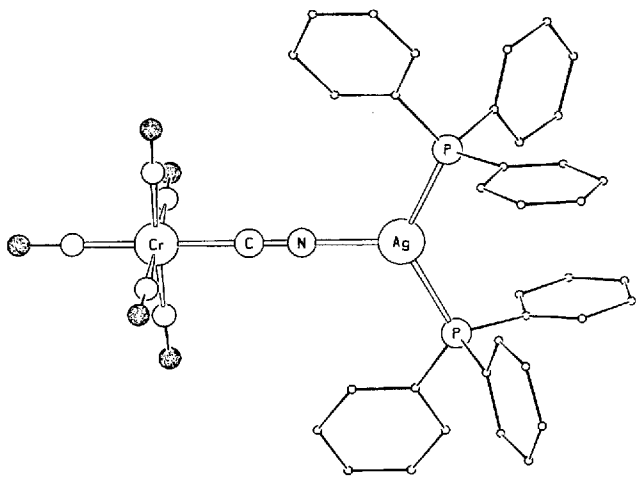

[a]Selected bond lengths [Å] and angles [°]: Cr–C1 2.01(2), Cr–C (CO-*trans*) 1.84(2), Cr–C (CO-*cis*, av.) 1.88(2), C1–N1 1.15(2), Ag–N1 2.17(2), Ag–P 2.440(2), Cr–C1–N1 180(0), Ag–N1–C1 180(0), N1–Ag–P1 116.97(6), P1–Ag–P1′ 126.07(1).

In complex **4** the Cr–C–N–Ag arrangement is seemingly linear due to the location of all four atoms on a crystallographic C2 axis. Despite the somewhat lower precision of the structure determination all bond distances around chromium or for the CN ligand resemble those in **2a**, **2b**,

and **3** again. The trigonal planar ligand arrangement around silver and the bond distances involved correspond to those in other $(Ph_3P)_2Ag$ complexes.[38] Altogether it can be stated that the various "organometallic isocyanides" CN−M′ impose very similar structural effects on the $(CO)_5Cr$ moiety.

IR Spectroscopy

The ν(CO) and ν(CN) absorptions of all complexes are given in the Experimental Section. The ν(CN) band of the neutral complexes is of low to extremely low intensity. Both the carbonyl and the cyanide vibrations provide useful information about the structural and bonding characteristics of the CN bridged species.

The information from ν(CO) data can be extracted from Table 2 which compares complexes containing the $(CO)_5Cr$ unit. The dinuclear complexes in the table are arranged in the order of decreasing $\nu(A_1^1)$ of the $(CO_5)Cr$ group which corresponds to the vibration of the *trans*-CO ligand which best reflects the bonding interactions between chromium and the attached M′−CN or M′−NC group. The data are also analyzed in terms of the ν(CO) force constants obtained with the Cotton-Kraihanzel method.[39] Table 2 shows that the simple approach of looking only at the $\nu(A_1^1)$ value and the computational approach of analyzing the data for Δk lead to the same ordering. Both a low $\nu(A_1^1)$ and a high Δk indicate a low π-acceptor strength/σ-donor strength ratio of the ligand attached to the $(CO)_5Cr$ moiety. The four reference ligands at the top of Table 2 qualify the organometallic ligands below. It is obvious that the organometallic isocyanides in **1a**, **2a**, **3**, and **4** act as π-acceptors similar to acetonitrile, but slightly weaker. In fact, they can be arranged between acetonitrile and the cyanide ion, which means that they are of medium-to-low π-acceptor strength. Among them the ordering corresponds to increasing electron richness as expressed by the number of donor ligands (PR_3, Cp) on M′. The organometallic cyanides NC−Fe(CO)$_2$Cp, NC−Fe(dppe)Cp, and NC−Mn(CO)$_2$Cp$^-$ are clearly separated from the corresponding isocyanides, their π-acceptor/σ-donor capacity being comparable to that of a pure nitrogen donor like an amine. They are again ordered according to their electron-richness resulting from the dppe ligand or the negative charge. The clear separation of the ν(CO) bands between complexes with M−C and M−N coordination holds for the IR data of all complexes. It thereby allows a consistant picture of relative π-acceptor properties, charge distributions, and isomer identifications for the series.

Similar conclusions can be drawn from the ν(CN) IR data. The ν(CN) bands of the metallocyanides $(CO)_5Cr-CN^-$ (2096 cm^{-1}), $(CO)_5Mo-CN^-$ (2100 cm^{-1}), $(CO)_5W-CN^-$ (2103 cm^{-1}), Cp(CO)$_2$Mn−CN (2061 cm^{-1}), Cp(CO)$_2$Fe−CN (2119 cm^{-1}), and Cp(dppe)Fe−CN (2063 cm^{-1}) move by 20−50 cm^{-1} to higher wavenumbers upon formation of the dinuclear complexes. This results from the kinematic effect of constraining the CN motion by double attachment[40] as well as from the electronic effect of strengthening the C≡N bond by using anti-bonding σ* electrons for M−N coordination. Table 3 illustrates the resulting phenomena for a series of complexes chosen such as to eliminate the kinematic influence. The latter is meant to be achieved by using organometallic units of nearly identical shape and weight (Cp(CO)$_2$Fe/Cp(CO)$_2$Mn) on one side of the dinuclear complexes. Table 3 contains two series of isoelectronic complexes. In the electron-poor series, Cp(CO)$_2$Fe−CN−M′, the ν(CN) band position rises roughly proportional to the electron-pair acceptor strength of the building block M′. In the electron-rich series, Cp(CO)$_2$Mn−CN−M′ the sequence is different, indicating that additional factors become influential. This may be related to M−C-π back donation which is stronger in the manganese series. Thus an increase in ν(CN) due to N→M′ σ donation is partially compensated by a simultaneous C≡N bond weakening due to the increased M→C π donation. Neither here nor elsewhere is π-backbonding from M′ to the cyanide nitrogen necessary to explain the effects observed in the structures or the IR data.

Table 2. ν(CO) bands and Cotton-Kraihanzel force constants for $(CO)_5Cr$ complexes with CN-containing ligands

L in $Cr(CO)_5L$	$\nu(A_1^1)$	k_2	k_1	Δk
CN^- [a]	1885	15.59	14.51	1.08
CNMe [a]	1964	16.10	15.75	0.35
NCMe [a]	1930	16.04	15.22	0.82
$NH_2C_6H_{11}$ [a]	1890	15.78	14.58	1.20
CN−FeCp(CO)$_2$ (**1a**)	1911	15.77	14.94	0.83
CN−Ni(PPh$_3$)Cp (**3**)	1905	15.69	14.83	0.86
CN−Ag(PPh$_3$)$_2$ (**4**)	1900	15.64	14.74	0.90
CN−Fe(dppe)Cp (**2a**)	1898	15.66	14.71	0.95
NC−Fe(CO)$_2$Cp (**1b**)	1884	15.78	14.50	1.28
NC−Fe(dppe)Cp (**2b**)	1869	15.69	14.26	1.43
NC−Mn(CO)$_2$Cp$^-$ [b]	1855	15.75	14.16	1.59

[a] Data from ref.[39] – [b] Data from ref.[23].

Table 3. ν(CN) values [cm^{-1}] for two series of isoelectronic dinuclear complexes Cp(CO)$_2$M−CN−M′

M′	ν(CN) for M = Fe	ν(CN) for M = Mn
–	2119	2061
Fe(dppe)Cp$^+$	2138	2087
Mn(CO)$_2$Cp	2147	2110[a]
W(CO)$_5$	2151	2100[a]
Fe(CO)$_2$Cp$^+$	2165	2095

[a] Data from ref.[23]

An inspection of the ν(CN) data of the five pairs of isomeric complexes leads to the same conclusions, cf Table 4. Firstly, the most electron rich species [i.e., the complexes containing Cp(CO)$_2$Mn or Cp(dppe)Fe] show the lowest ν(CN) values. Secondly, within the pairs the one which has the cyanide carbon attached to the more electron rich unit has the lower ν(CN). Thereby again a structural assignment of the isomers can be made which agrees with that from the synthetic pathway or from the ν(CO) data. Thus, although being more complex in nature, the ν(CN) band positions lead to interpretations which are complementary to those

of the ν(CO) band positions and thereby quantify the net electron flow across the bridging cyanide ligand.

Table 4. Comparison of ν(CN) [cm^{-1}] for isomeric complexes

complex pair	isomer **a**	isomer **b**
$(CO)_5Cr[\mu\text{-}CN]Fe(CO)_2Cp$ (**1**)	2132	2157
$(CO)_5Cr[\mu\text{-}CN]Fe(dppe)Cp$ (**2**)	2115	2103
$(CO)_5W[\mu\text{-}CN]Fe(CO)_2Cp$ (**9**)	2134	2151
$Cp(CO)_2Fe[\mu\text{-}CN]Mn(CO)_2Cp$ (**12**)	2147	2094
$Cp(dppe)Fe[\mu\text{-}CN]Mn(CO)_2Cp$ (**15**)	2105	2087

Electrochemistry

14 of the 21 new complexes yielded satisfactory cyclic voltammograms. The redox potentials obtained are listed in Table 5 together with some reference data of related mononuclear cyanide complexes. Taking the $E_{1/2}$(ox1) potentials of the mononuclear metallocyanides as a measure of the electron density on the organometallic unit, one comes up with the same ranking as from the ν(CO) data (Table 2) and with a ranking very close to that from the ν(CN) data (Table 3). Based on this it can be predicted on which of the two organometallic units in the dinuclear complexes an oxidation or reduction will take place.

Table 5. Cyclovoltammetric data [V] of mononuclear metallocyanides and dinuclear complexes[a]

complex	$E^{1/2}$(red)	$E^{1/2}$(ox 1)	$E^{1/2}$(ox 2)
$(CO)_5Cr-CN^-$	–	+0.58	–
$Cp(CO)_2Mn-CN^-$	–	+0.11	–
$Cp(CO)_2Fe-CN^-$	–	+1.8(irr)	–
$Cp(dppe)Fe-CN$	–	+0.48	–
$Cp(PPh_3)_2Ru-CN$	–	+0.79	–
1a	−1.34(irr)	+0.80	–
1b	−1.70(irr)	+0.68	–
2a	–	+0.28	+0.97
2b	–	+0.46	+0.91
6	–	+0.30	+1.13(irr)
8	–	+0.32	+1.17(irr)
11	−0.91(irr)	+1.72(irr)	–
12a	–	+0.02	–
12b	–	+0.24	–
13	–	+0.46	–
14	–	+0.25	+1.12(irr)
15a	–	+0.18	+0.70
15b	–	0.00	+0.61
16	–	+0.31	+1.32

[a] Measured in CH_2Cl_2 against Ag/AgCl, scan speed 100 mV/s; irr = irreversible.

While there was not much reductive chemistry, all but one of the dinuclear complexes showed a reversible one-electron oxidation, and the more electron-rich ones could be oxidized a second time. The potentials for the first oxidations fall in typical ranges. They are lowest for complexes containing $Cp(CO)_2Mn$, followed by Cp(dppe)Fe. Of the isomers that with the more electron-rich unit bound to nitrogen is 0.1−0.2 V easier to oxidize than the other one. A comparison of the complexes containing *N*-bound Fe(dppe)Cp (**2a**, **6**, **8**, **13**, **14**) shows that the other organometallic unit has a small influence on the redox potential which, however, is typically related to its charge and electron density. A similar trend, but with a larger variation of $E^{1/2}$, is observed when comparing the influence of the other organometallic unit in the $Cp(CO)_2Mn-CN$ derivatives **12b** and **15b** or the Cp(dppe)Fe−CN derivatives **2b**, **15a**, and **16**.

Due to the ability of the bridging cyanide ligand to transfer charge between the two organometallic units the electrochemical data give no unambiguous information about the location of the charge after oxidation. In some cases ESR spectroscopy might be helpful here. But room temperature ESR spectra of some of the isolated oxidized complexes in CH_2Cl_2 solution showed only unstructured and very broad (several hundred Gauss) ESR signals. Similarly a comparison of the intervalence transfer bands (see below) of two linkage isomers of an oxidized complex would help clarify the location of charge and the direction of charge transfer. Again this has not been possible because two such isomers could not be isolated yet.

Chemical Oxidations

All dinuclear complexes were subjected to one-electron oxidation by $[Cp_2Fe]PF_6$ or $[(p\text{-}BrC_6H_4)_3N]BF_4$. But only six of these reactions resulted in the isolation of stable products. All six belong to the group of complexes which were also susceptible to electrochemical oxidation (see Table 5). To our surprise the $Cp(CO)_2Mn$ containing complexes **12a**, **b** and **15a**, **b** which have quite low redox potentials could not be isolated as cations. This, however, corresponds with the inaccessibility of the neutral oxidation product from anionic $[Cp(CO)_2Mn-CN-Mn(CO)_2Cp]^-$ ($E_{1/2}$ − ox = +0.11 V).[23] The isolated products are:

$[(CO)_5Cr-CN-Fe(dppe)Cp]BF_4$ **2a-ox**

$[(CO)_5Mo-CN-Fe(dppe)Cp]BF_4$ **6-ox**

$[(CO)_5W-CN-Fe(dppe)Cp]BF_4$ **8-ox**

$[Cp(CO)_2Fe-CN-Fe(dppe)Cp](PF_6)_2$ **13-ox**

$[Cp(CO)(CN)Fe-CN-Fe(dppe)Cp]PF_6$ **14-ox**

$[Cp(PPh_3)_2Ru-CN-Fe(dppe)Cp](PF_6)_2$ **16-ox**

All six isolated complexes contain the *N*-bound Fe(dppe)Cp unit which, together with the $Mn(CO)_2Cp$ unit, is the most electron-rich of the units employed here. This indicates that the redox reaction takes place at this unit and that it is inert enough in the oxidized paramagnetic state. In contrast, the $Cp(CO)_2Mn$ containing complexes including mononuclear $Cp(CO)_2Mn-CN^-$ [23] seem to be labile against ligand dissociation or disproportionation after oxidation. Each of them was easily and quickly oxidized by $[Cp_2Fe]PF_6$, but the observed colour changes of their solutions disappeared soon, and after that IR spectra of the solutions indicated only the presence of the neutral starting complexes.

Complex **2a-ox** was chosen for a structure determination in order to get a comparison with the structures of **2a** and **2b**. Figure 4 shows the result. A comparison with Figure 1 reveals that the overall shapes of the oxidized and neutral complexes are very similar and that there are only slight rotational differences for the phenyl groups with respect to

the P–C bonds and for the $Cr(CO)_5$ unit with respect to the Cr–CN–Fe line.

Figure 4. Molecular structure of the cation of **2a-ox**[a]

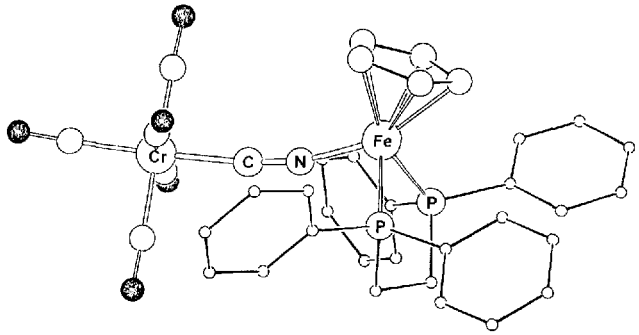

[a] Selected bond lengths [Å] and angles [°]: Fe–N1 1.892(8), Fe–P1 2.267(3), Fe–P2 2.251(3), Cr–C1 1.998(11), Cr–C(CO-*trans*) 1.87(2), Cr–C(CO-*cis*, av.) 1.88(2), C1–N1 1.137(11), Cr–C1–N1 173.1(9), Fe–N1–C1 165.2(8).

All molecular details also differ only slightly between **2a** and **2a-ox**. The Fe–N bond in **2a-ox** is 0.04 Å shorter while the Fe–P and Fe–C(Cp) bonds are, on the average, 0.06 and 0.03 Å longer. This corresponds to the location of the positive charge on the iron atom, to the reduced back-bonding from iron to the phosphane and Cp ligands, and it supports the statement that the cyanide N atom has no noticeable π-acceptor properties. On the other side the Cr–C(CN) bond is 0.06 Å shorter and the Cr–C(CO-*trans*) bond is 0.03 Å longer in **2a-ox** than in **2a**. This clearly indicates that the removal of electron density from the iron atom has significantly increased the π-acceptor properties of the cyanide carbon atom. The C–N distance in **2a-ox** is just 0.02 Å less than that in **2a** which, when compared to the large change in ν(CN) (see below), again tells that there is no diagnostic value in C–N distances. The deviaton of the Cr–C–N–Fe arrangement in **2a-ox** from linearity is comparable to those in **2a** and **2b**: again the M–N–C part shows a stronger bending (15°) than the M–C–N part (7°).

IR Data and Magnetism of Oxidized Complexes

Upon oxidation of the complexes the IR bands for the CN stretch move to considerably lower wavenumbers and become as strong as the ν(CO) bands which in turn move to slightly higher wavenumbers (details see Experimental Section). This created ambiguities in the assignment of the bands which were resolved for the $M(CO)_5$ containing complexes by calculating the Cotton-Kraihanzel force constants for different assignments of the ν(CO) bands and picking those which produced higher k values [corresponding to reduced M–C(CO) backbonding] for the oxidized in comparison to the neutral complexes. Table 6 lists and compares the ν(CN) values.

The oxidation of the Cp(dppe)Fe unit at the N terminus induces a net flow of electron density from the *C*-bound unit into the CN ligand which increases its polarity and thereby increases the oscillator strength of its CN vibration. This corresponds to increased π-backdonation from the *C*-bound metal unit which reduces the strength of the C≡N bond. At the same time there is less π-backdonation available for the CO ligands on the *C*-bound metal unit and hence their C≡O bonds become stronger. Similar phenomena have been observed before for cyanide bridged species of the types $[L_3(CO)_2Mn–CN–Mn(CO)_2L'_3]^{2+}$ and $[Cp(PPh_3)_2Ru–CN–Ru(NH_3)_5]^{3+}$.[11][18] The compounds described here have provided the added advantage of allowing the isolation of a series of oxidized species with a high transduction of electron density as visible from the Δν values in Table 6. This in turn confirms that the interpretation of their electronic situation is consistent with the data from molecular structures, infrared and electrochemical data as well as from the electronic spectra (see below).

Table 6. Cyanide stretches [cm^{-1}] for neutral and oxidized dinuclear complexes

M in M–CN–Fe(dppe)Cp	ν(neutral)	ν(ox)	Δν
$(CO)_5Cr$ (**2a**)	2115	2011	−104
$(CO)_5Mo$ (**6**)	2114	2021	−93
$(CO)_5W$ (**8**)	2115	2016	−99
$Cp(CO)_2Fe^-$ (**13**)	2141	2116	−25
Cp(CO)(CN)Fe (**14**)	2118	2056	−62
$Cp(PPh_3)_2Ru^+$ (**16**)	2069	1996	−73

Complexes **13** and **16** as well as their oxidation products **13-ox** and **16-ox** were subjected to magnetic measurements at room temperature. The results are listed in Table 7. The amount of diamagnetism observed for **13** and **16** was applied as a correction to the magnetic susceptibilities of **13-ox** and **16-ox**. The resulting magnetic moments are in good agreement with the value of 1.73 BM expected for one unpaired electron. The value of the investigated organometallic species in this respect lies in the availability of the diamagnetic reference compounds. This should facilitate the evaluation of magnetic interactions in similar oligonuclear species which after oxidation have more than one unpaired electron.

Table 7. Magnetic measurements[a]

complex	χ_{mol}	χ_{mol}^{corr}	μ_{eff}
13	−0.17	–	–
13-ox	+1.19	1.36	1.78
16	−0.49	–	–
16-ox	+0.69	1.18	1.66

[a] χ_{mol} in 10^{-3} cm^3mol^{-1}; $\mu_{eff} = 2.828\sqrt{(\chi_{mol} \cdot T)}$, T = 293 K.

Electronic Spectra

Cyanide-bridged complexes with mixed redox states are expected to show metal-to-metal charge transfer (MMCT) bands in their electronic spectra. This has been observed for dinuclear complexes,[15][18] but not typically for organometallic ones.[11][41] The oxidized complexes obtained here, with the exception of **13-ox**, give rise to very strong MMCT bands in the visible to near-infrared region. Table

8 lists the values, and Figure 5 demonstrates the effects by comparing **2a** and **2a-ox**.

Table 8. Electronic spectra of oxidized complexes[a]

complex	λ_{max} [nm]	λ_{max} [l M^{-1} cm^{-1}]	$\Delta\nu_{1/2}$ [cm^{-1}][b]	α^{2}[c]
2a-ox	1130	5400	3930	0.041
6-ox	1080	4000	3870	0.028
8-ox	1030	4800	3990	0.034
14-ox	880	1200	3900	0.007
16-ox	690	3700	5660	0.025

[a] Measured in CH_2Cl_2. – [b] Band width at half intensity. – [c] Calculated as $\alpha^2 = 4.24 \cdot 10^{-4} \cdot (\varepsilon_{max}\Delta\nu_{1/2})/(G\nu_{max}R^2)$ with G (degeneracy) = 1 and R (M–M distance) = 5.0 Å.

Figure 5. Electronic absorptions of **2a** (---) and **2a-ox** (–), measured in CH_2Cl_2

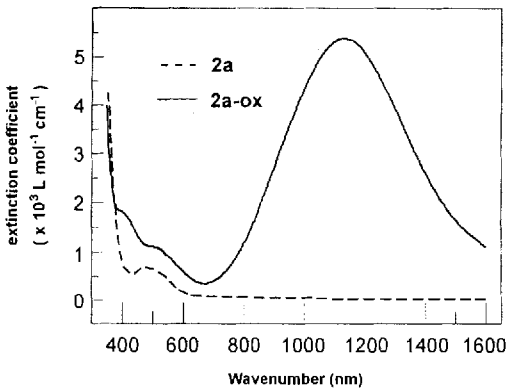

The band positions and intensities as well as the half widths classify the complexes as typical class II mixed-valence compounds according to the classification of Robin and Day.[42] This is borne out by the values of the electron delocalization parameter α^2 (see Table 8) as calculated according to the simplified Hush formalism[43] from ν_{max}, ε_{max}, and $\Delta\nu_{1/2}$. The α^2 values are actually quite high in comparison to those of other cyanide bridged systems, which corresponds with the CN-mediated electron flow between the two metal centers as evidenced by the very significant lowering of the ν(CN) values upon oxidation. The only exception to this rule seems to be complex **14-ox** which has an additional cyanide ligand which obviously causes a different electron distribution in the oxidized complex as evidenced by the unusually low extinction of the MMCT absorption.

The electronic spectra yield further information with respect to the electronic nature of the oxidized complexes and its variability. Thus the band positions of the MMCT bands (i.e., their energies expressed as ν in cm^{-1}) are proportional to the redox potentials of the metallocyanides M–CN attached to the Cp(dppe)Fe unit. This can be seen by comparing the top entries in Table 5 with the first column in Table 8. This clearly indicates that the metal-to-metal charge transfer is from the other organometallic unit to the Cp(dppe)Fe unit. It may also explain why no MMCT band was observed for **13-ox**: the redox potential for $Cp(CO)_2$-Fe–CN is so high that the MMCT absorption may be hidden under other bands in the visible region or even shifted into the UV range.

The solvent dependency of the MMCT demonstrates that the energy difference of the electronic states on both metal centers, rather than the reorganization energy, dominates the energies of the transitions, as with other systems.[18][44] Complex **2a-ox** was chosen for the measurements. When the solvent donicity is increased the MMCT requires higher energies, the extinction coefficient of the MMCT bands gets smaller, and the bands get broader. Table 9 lists the measurements. A close-to-linear correlation can be obtained between Gutmann's solvent donor numbers[45][46] and the MMCT energies, as presented in Figure 6 in terms of band positions expressed in cm^{-1}. The least-squares line has a slope of 102 cm^{-1}/DN which is similar to the slope of 129 cm^{-1}/DN observed for $[Cp(PPh_3)_2Ru-CN-Ru(NH_3)_5]^{3+}$.[18] This positive solvatochromic effect implies that the ground state is more stabilized by solvation than the excited state. This in turn means that the $Cp(dppe)Fe^+$ unit is more amenable to outer sphere solvent coordination than a neutral or cationic $Cr(CO)_5$ unit.

Table 9. Solvent dependency of MMCT transitions and CO and CN vibrations for **2a-ox**

solvent	DN[a]	λ_{max} [nm]	ν(CN) [cm^{-1}]	ν(CO)[b] [cm^{-1}]
CH_2Cl_2	1.0	1130	2011	1949
C_6H_5Cl	3.3	1035	2015	1947
$C_6H_5NO_2$	4.4	1010	2019	1948
CH_3CN	14.1	930	2025	1948
acetone	17.0	920	–	–
DMF	26.6	850	2031	1945

[a] Solvent donor number.[45] – [b] E band + A_1^1 band.

Figure 6. Dependency of the MMCT energy of complex **2a-ox** upon solvent donicity

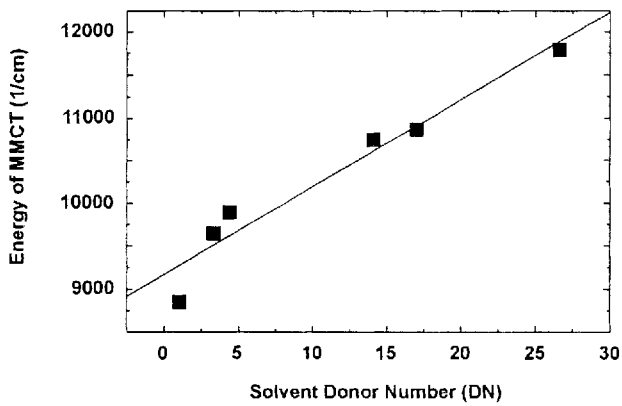

The latter is borne out by the IR data, cf. Table 9. It can be seen that the position of the ν(CN) band responds significantly to a change in solvent donicity in the required direction, i.e. a donor stabilization of the $Cp(dppe)Fe^+$ unit requires less flow of electron density from the $(CO)_5Cr$ unit and hence less weakening of the C≡N bond. For comparison the ν(CO) and ν(CN) bands in neutral **2a** do not respond to solvent changes, and neither does the strong ν(CO) band of **2a-ox** (the weak ν(CO) band in the 2080

cm^{-1} region is difficult to assign in a region of strong solvent absorption). Figure 7 displays the very good proportionality between the solvent dependencies of ν(CN) and ν(MMCT) as a final demonstration of the consistency of observations and interpretations obtained by this study.

Figure 7. Relationship between ν(CN) (IR spectra) and ν(MMCT) (electronic spectra) of complex **2a-ox** upon variation of the solvent

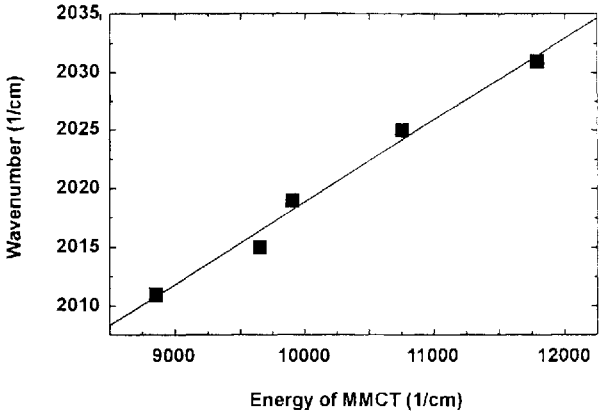

Conclusions

The ease of synthesis and chemical inertness of cyanide-bridged organometallic dinuclear complexes have made a large number of new complexes available. This in turn has allowed a comprehensive and comparative study of their properties with structural, spectroscopic, and redox methods. The results of this study confirm and complement those of previous studies but exceed them in depth, variability, and consistency. The main findings are:

1. The synthetic method allows the combination of organometallic units spanning the whole transition metal series (Cr to Ag). The orientation of the cyanide bridge (M−CN−M′ vs. M−NC−M′) is predetermined by the choice of reagents. Several pairs of linkage isomers were obtained as well as several groups of isoelectronic dinuclear species.

2. The molecular structures of the dinuclear complexes display close to linear M−C−N−M′ arrangements. The interpretations of bonding derived from bond distances and angles correspond to expectation, but all observed effects are small. Specifically the complex $(CO)_5Cr(\mu$-CN)Fe(dppe)Cp has made possible for the first time a structural comparison of the M−CN−M′, M−NC−M′, and $[M-CN-M']^+$ situations showing that the three complexes are nearly superimposable.

3. IR data in the CO as well as in the CN region are a reliable indicator of relative electron donator and acceptor strengths of the two organometallic units and of their mutual dependency. They allow an identification of the cyanide *C*- and *N*-bound units and a distinction of the linkage isomers. Their variation upon oxidation of the complexes yields valuable information about the bonding situation in the oxidized species.

4. All complexes are electrochemically active, showing at least one one-electron oxidation. The chemical stability of the oxidized species is such that only those with cyanide *N*-bound Fe(dppe)Cp units can be isolated. The redox potentials depend in a characteristic fashion on the electron-richness of the organometallic units and on their mode of attachment (C or N) to the cyanide bridge.

5. The oxidized dinuclear complexes exhibit strong MMCT absorptions in the visible or near-IR regions. Analysis of the electronic spectra qualifies the complexes as class II mixed valence species. The energies required for MMCT are correlated with the redox potentials of the M−CN constituents of the dinuclear complexes. They are solvent dependent. Their linear relation with the solvent donicity and with the CN stretching frequency point to a ground-state stabilization by interaction between the Fe(dppe)Cp unit and the donor molecules.

Altogether these findings have verified our expectation that organometallic metallocyanides should have a rich oligonuclear complex chemistry and that they should yield physical phenomena which are the molecular level analogues of the properties of Prussian Blue. Thus they have motivated us to continue this work with higher nuclearity species and with compounds containing more unpaired electrons.

This work was supported by the *Deutsche Forschungsgemeinschaft*, the *European Commission*, and by the *Fonds der Chemischen Industrie*. We thank Prof. *J. Heinze* and Prof. *D. Siebert* for help with the electrochemical and ESR measurements.

Experimental Section

All manipulations were performed under dry nitrogen using standard Schlenk and syringe techniques. The solvents were dried by reflux over the appropriate drying agents (CH_2Cl_2 and NCMe/drying reagent CaH_2; NCEt, ether, acetone, and DMF/4-Å molecular sieves; pentane, hexane, THF, benzene, and toluene/Na-K alloy; CH_3OH/Mg; 2-propanol/Na) and distilled prior to use.

Photochemical reactions were carried out under nitrogen using a mercury high-pressure burner of type Hanau TQ 150-Z3. The silica gel for column chromatography (Machery-Nagel silica gel 60, 0.063−0.2 mm) was dried in vacuo at ca. 150°C for min 8 h before use. The solvent mixture used for chromatography was chosen by a preceding thin layer chromatography which was performed on Merck silica gel 60 F_{254}, thickness 0.2 mm.

IR spectra (in CH_2Cl_2, cm^{-1}): Bruker FT-IR Spectrometer IFS-25. − ^{1}H-NMR spectra (in $CDCl_3$, int. TMS, δ): Bruker AC-200. − UV/Vis/NIR spectra: JASCO-UV-570 instrument (range from 200 nm to 2500 nm). − Magnetic susceptibilities: MSB-Auto balance at room temperature. − Cyclic voltammetry (CV): Amel-5000 system using Ag/AgCl as reference electrode, the counter and working electrodes were platinum, tetra(*n*-butyl)ammonium hexaflurophosphate (TBAFP) was used as electrolyte. − The solvents CH_2Cl_2 or CH_3CN were purified before use. Cobaltocenium hexaflurophosphate, octamethylferrocene, or ferrocene were used as internal standards, which have the potentials of −0.94 (−0.98), −0.01 (−0.05) or +0.39 (+0.35) V in CH_2Cl_2 (CH_3CN) against Ag/AgCl, respectively.

Starting Materials: PPN[CN],[47] $(CO)_5M(THF)$ (M = Cr, Mo, W),[48] $CpMn(CO)_2(THF)$,[49] $Na[NCM(CO)_5]$ (M = Cr, Mo, W),[50] $Na[NCMn(CO)_2Cp]$,[51] $K[(NC)_2Fe(CO)Cp]$,[52] $Cp(CO)_2$-FeCN,[53] Cp(dppe)FeCN,[54] $Cp(PPh_3)_2RuCN$,[54] $(PPh_3)_2Ag$-

(NO_3),[55] $Cp(PPh_3)NiCl$,[56] $[Cp(CO)_2Fe(THF)](BF_4)$,[57] Cp(dppe)FeBr,[58] and $Cp(PPh_3)_2RuCl$[59] were prepared as described.

Dinuclear Complexes

1a: To a mixture of 0.168 g (0.50 mmol) of $[Cp(CO)_2Fe\cdot THF]BF_4$ and 0.120 g (0.50 mmol) of $NCCr(CO)_5]$ was added 10 ml of CH_2Cl_2 and the solution stirred for 20 min. TLC showed a single orange band. The reaction solution was chromatographed on a 5 × 1.5 cm silica-gel column using CH_2Cl_2 as eluent. A single orange band was collected. The solvent was removed under reduced pressure to leave an orange residue. The residue was redissolved in 5 ml of CH_2Cl_2 and then layered with 20 ml of hexane. The mixture was kept at −20°C for two days. The crystals were filtered off, washed with 5 ml of hexane for 2 times and dried in vacuo. This yielded 0.10 g (51%) of **1a** as orange crystals, m.p.: 133°C (dec.). − IR [cm^{-1}]: $\tilde{\nu}$ = 2132w (CN), 2070m, 2057m, 2023m, 1934s, 1905sh (CO). − ^1H NMR: δ = 5.13 (s, Cp). − $C_{13}H_5CrFeNO_7$ (395.03): calcd. C 39.53, H 1.28, N 3.55; found C 39.49, H 1.26, N 3.54.

1b: A solution of 0.110 g (0.50 mmol) of $Cr(CO)_6$ in 100 ml of THF was UV-irradiated for 0.5 h which formed a yellow solution containing $Cr(CO)_5(THF)$. To the yellow solution was added solid 0.103 g (0.50 mmol) of $CpFe(CO)_2CN$. The resulting solution was stirred for 0.5 h. The solvent was removed under reduced pressure to leave a yellow residue. The yellow residue was chromatographed on a 5 × 1.5 cm silica-gel column using CH_2Cl_2 as eluent. A single yellow band moved and was collected. The solvent was removed under reduced pressure. The residue was redissolved in 6 ml of CH_2Cl_2 and layered with 30 ml of hexane. The mixture was kept at 4°C for two days. The yellow crystals were filtered off, washed with 5 ml of hexane for 2 times and dried in vacuo. This yielded 0.13 g (66%) of **1b** as yellow crystals, m.p.: 138°C (dec.). − IR [cm^{-1}]: $\tilde{\nu}$ = 2157w (CN), 2071w, 2062m, 2021m, 1933s, 1883m (CO). − ^1H NMR: δ = 5.14 (s, Cp). − $C_{13}H_5CrFeNO_7$ (395.03): calcd. C 39.53, H 1.28, N 3.55; found C 39.38, H 1.11, N 3.40.

2a: To a mixture of 0.092 g (0.38 mmol) of $Na[NCCr(CO)_5]$ and 0.229 g (0.38 mmol) of Cp(dppe)FeBr was added 10 ml of CH_2Cl_2 and the solution stirred for 30 min. The resulting red solution was chromatographed on a 5 × 1.5 cm silica-gel column using CH_2Cl_2 as eluent. A single red band moved and was collected. The solvent was removed under reduced pressure. The residue was redissolved in 6 ml of CH_2Cl_2 and layered with 25 ml of hexane. The mixture was left at −27°C for two days. The crystals were filtered off, washed with 5 ml of hexane for 2 times and dried in vacuo. Yield 0.26 g (93%) of **2a** as red crystals, m.p.: 176°C (dec.). − IR [cm^{-1}]: $\tilde{\nu}$ = 2115w (CN), 2056w, 1930s, 1898m (CO). − ^1H NMR: δ = 7.1−8.0 (m, 20 H, Ph), 4.16 (s, 5 H, Cp), 2.45−2.50 (m, 4 H, C_2H_4). − $C_{37}H_{29}CrFeNO_5P_2$ (737.43): calcd. C 60.26, H 3.96, N 1.90; found C 59.50, H 3.96, N 1.84.

2b: A solution of 0.110 g (0.5 mmol) of $Cr(CO)_6$ in 120 ml of THF was UV-irradiated for 40 min to form a yellow solution containing $(CO)_5Cr(THF)$. To the yellow solution was added a solution of 0.270 g (0.50 mmol) of CpFe(dppe)CN in 10 ml of CH_2Cl_2. The resulting solution was stirred for 5 min. The solvent was removed under reduced pressure to leave a yellow residue. The residue was chromatographed on a 5 × 1.5 cm silica-gel column using CH_2Cl_2 as eluent. A single yellow band moved and was collected. The solvent was removed under reduced pressure, and the residue redissolved in 6 ml of CH_2Cl_2 and layered with 30 ml of hexane. After three days the crystals were filtered off, washed with 5 ml of hexane for 2 times and dried in vacuo. This yielded 0.230 g (62%) of **2b** as yellow crystals, m.p.: 135°C (dec.). − IR [cm^{-1}]: $\tilde{\nu}$ = 2103w (CN), 2064w, 1928s, 1869m (CO). − ^1H NMR: δ = 7.1−7.9 (m, 20 H, Ph), 4.22 (t, J = 1.3 Hz, 5 H, Cp), 2.45−2.50 (m, 4 H, C_2H_4). − $C_{37}H_{29}CrFeNO_5P_2$ (737.43): calcd. C 60.26, H 3.96, N 1.90; found C 58.71, H 3.92, N 1.78.

3: To a solution of 340 mg (0,50 mmol) of $Cp(PPh_3)NiCl$ in 10 ml of CH_2Cl_2 was added a solution of 380 mg (0,50 mmol) of $PPN[NCCr(CO)_5]$ in 5 ml of CH_2Cl_2 and the mixture stirred for 2 h. The color of the reaction solution changed to dark-brown. The resulting solution was concentrated to 2 ml and chromatographed on a 10x1.5 cm silica-gel column using CH_2Cl_2 as eluent. The first brown band was collected. After evaporation of the solvent the residue was redissolved in 20 ml of benzene and 50 ml of hexane was added. The mixture was kept at −27°C for 3 d. After filtration, washing with 5 ml of hexane for three times and drying in vacuo, the yield was 0.165 g (54%) of **3** as dark-brown crystals, m.p.: 110°C (dec.). − IR [cm^{-1}]: $\tilde{\nu}$ = 2127w (CN), 2057w, 1968sh, 1934s, 1905sh (CO). − ^1H NMR: δ = 7.4−7.8 (m, 15 H, Ph), 5.19 (s, 5 H, Cp). − $C_{29}H_{20}CrNNiO_5P$ (604.14): calcd. C 57.66, H 3.34, N 2.32; found C 57.75, H 3.42, N 2.35.

4: To a solution of 0.140 g (0.20 mmol) of $(PPh_3)_2AgNO_3$ in 5 ml of CH_2Cl_2 was added dropwise a solution of 0.150 g (0.20 mmol) of $PPN[NCCr(CO)_5]$ in 5 ml of CH_2Cl_2 and the mixture stirred for 20 min. The solution was concentrated to 2 ml and filtered through a 3 × 1.5 cm silica-gel column with 50 ml of CH_2Cl_2:hexane (1:1). The solvent was removed under reduced pressure to leave a white residue. The residue was redissolved in 4 ml of CH_2Cl_2 and layered with 20 ml of ethanol. This yielded 0.070 g (40%) of **4** as colorless crystals. − IR [cm^{-1}]: $\tilde{\nu}$ = 2110w (CN), 2054w, 1931s, 1900sh (CO). − ^1H NMR: δ = 7.3−7.8 (m, Ph). − $C_{42}H_{30}NAgCrO_5P_2$ (850.52): calcd. C 59.31, H 3.56, N 1.65; found C 59.03, H 3.55, N 1.60.

5: The same procedure as for **1a** was used except using 0.17 g (0.50 mmol) of $[Cp(CO)_2Fe\cdot THF]BF_4$ and 0.14 g (0.50 mmol) of $Na[NCMo(CO)_5]$. Yield 0.10 g (48%) of **5** as ochre crystals, m.p.: 128°C (dec.). IR [cm^{-1}]: $\tilde{\nu}$ = 2131w (CN), 2071m, 2061m, 2024m, 1936s, 1900sh (CO). ^1H NMR: δ = 5.14 (s, Cp). $C_{13}H_5NFeMoO_7$ (438.97): calcd. C 35.57, H 1.15, N 3.13; found C 35.42, H 1.07, N 3.08.

6: The same procedure as for **2a** was used except using 0.200 g (0.33 mmol) of Cp(dppe)FeBr and 0.095 g (0.33 mmol) of $Na[NCMo(CO)_5]$. Yield 0.237 g (91%) of **6** as red crystals, m.p. 178°C (dec.). − IR [cm^{-1}]: $\tilde{\nu}$ = 2114vw (CN), 2062w, 1975w, 1932s, 1897m (CO). − ^1H NMR: δ = 7.1−7.9 (m, 20 H, Ph), 4.16 (s, 5 H, Cp), 2.45−2.50 (m, 4 H, C_2H_4). − $C_{37}H_{29}NFeMoO_5P_2$ (781.38): calcd. C 56.87, H 3.74, N 1.79; found C 56.58, H 3.69, N 1.74.

7: The same procedure as for **3** was used except using 105 mg (0.25 mmol) of $Cp(PPh_3)NiCl$ and 71 mg (0.25 mmol) of $Na[NCMo(CO)_5]$. Yield 0.15 g (95%) of **7** as black crystals, m.p.: 120°C (dec.). − IR [cm^{-1}]: $\tilde{\nu}$ = 2140w (CN), 2070w, 1935s, 1879m (CO). − ^1H NMR: δ = 7.4−7.7 (m, 15 H, Ph), 5.23 (s, 5 H, Cp). − $C_{29}H_{20}NMoNiO_5P$ (648.09): calcd. C 53.75, H 3.11, N 2.16; found C 53.61, H 3.09, N 2.18.

8: The same procedure as for **2a** was used except using 0.200 g (0.33 mmol) of Cp(dppe)FeBr and 0.124 g (0.33 mmol) of $Na[NCW(CO)_5]$. Yield 0.262 g (90%) of **8** as red crystals, m.p. 156°C (dec.). − IR [cm^{-1}]: $\tilde{\nu}$ = 2115vw (CN), 2060w, 1965w, 1924s, 1894m (CO). − ^1H NMR: δ = 7.0−7.9 (m, 20 H, Ph), 4.16 (s, 5 H, Cp), 2.40−2.45 (m, 4 H, C_2H_4). − $C_{37}H_{29}NFeO_5P_2W$ (869.29): calcd. C 51.12, H 3.36, N 1.61; found C 50.67, H 3.32, N 1.73.

9a: The same procedure as for **1a** was used except using 0.336 g (1.0 mmol) of $[Cp(CO)_2Fe\cdot THF]BF_4$ and 0.373 g (1.0 mmol) of $Na[NCW(CO)_5]$. Yield 0.35 g (66%) of 9a as ochre crystals, m.p.:

128°C (dec.). – IR [cm^{-1}]: $\tilde{\nu}$ = 2134w (CN), 2071m, 2059m, 2024m, 1929s (CO). – ^1H NMR: δ = 5.15 (s, Cp). – $C_{13}H_5NFeO_7W$ (526.88): calcd. C 29.63, H 0.96, N 2.66; found C 29.53, H 0.89, N 2.59.

9b: The same procedure as for **1b** was used except using 0.352 g (1.0 mmol) of $W(CO)_6$ in 120 ml of THF, (UV-irradiated for 1.5 h) and 0.205 g (1.0 mmol) of $CpFe(CO)_2CN$. Yield 0.28 g (53%) of **9b** as yellow crystals, m.p.: 124°C (dec.). – IR [cm^{-1}]: $\tilde{\nu}$ = 2151w (CN), 2072w, 2063m, 2023m, 1926s, 1880m (CO). – ^1H NMR: δ = 5.12 (s, Cp). – $C_{13}H_5NFeO_7W$ (526.88): calcd. C 29.63, H 0.96, N 2.66; found C 29.85, H 0.82, N 2.56.

10: The same procedure as for **3** was used except using 105 mg (0.25 mmol) of $Cp(PPh_3)NiCl$ and 94 mg (0.25 mmol) of $Na[NCW(CO)_5]$. Yield 142 mg (77%) of **10** as dark-brown crystals, m.p.: 134°C (dec.). – IR [cm^{-1}]: $\tilde{\nu}$ = 2129w (CN), 2061w, 1970sh, 1929s, 1900sh (CO). – ^1H NMR: δ = 7.4–7.8 (m, 15 H, Ph), 5.20 (s, 5 H, Cp). – $C_{29}H_{20}NNiO_5PW$ (736.00): calcd. C 47.33, H 2.74, N 1.90; found C 47.61, H 2.82, N 1.86.

11: To a mixture of 127 mg (0.63 mmol) of $CpFe(CO)_2CN$ and 210 mg (0.63 mmol) of $[CpFe(CO)_2(THF)]BF_4$ was added 10 ml of CH_2Cl_2 and the solution stirred for 1 h. The color of the solution changed from red to yellow. The solvent was removed under reduced pressure. The residue was redissolved in 4 ml of CH_2Cl_2 and then 20 ml of isopropanol were added. The resulting solution was concentrated to about 20 ml, then left at −27°C for three days. The yellow crystals were filtered off, washed with 5 ml of hexane for 2 times and dried in vacuo. This yielded 140 mg (48%) of **11** as yellow crystals, m.p.: 154°C (dec.). – IR [cm^{-1}]: $\tilde{\nu}$ = 2165w (CN), 2069s, 2025s (CO). – ^1H NMR: δ = 5.31 (s, 5H), 5.29 (s, 5H). – $C_{15}H_{10}NBF_4Fe_2O_4$ (466.75): calcd. C 38.60, H 2.16, N 3.00; found C 38.46, H 1.97, N 3.00.

12a: A solution of 0.208 g (1.0 mmol) of $CpMn(CO)_3$ in 100 ml of THF was UV-irradiated for 3 h. A red solution containing $CpMn(CO)_2(THF)$ was formed. Then 0.205 g (1.0 mmol) of solid $CpFe(CO)_2CN$ was added and the solution stirred for 2 h. The solvent was removed under reduced pressure. The residue was chromatographed on a 5 × 1.5 cm silica-gel column using CH_2Cl_2 as eluent. A single red band moved and was collected. The solvent of the collected red solution was removed under reduced pressure. Then the residue was redissolved in 6 ml of CH_2Cl_2 and layered with 30 ml of hexane. After two days red crystals were formed which were filtered off, washed with 5 ml of hexane for 2 times and dried in vacuo. This yielded 0.082 g (22%) of **12a** as orange-red crystals, m.p.: 132°C (dec.). – IR [cm^{-1}]: $\tilde{\nu}$ = 2144vw (CN), 2054s, 2012s, 1907s, 1830s (CO). – ^1H NMR: δ = 5.07 (s, 5H), 4.41 (s, 5H). – $C_{15}H_{10}NFeMnO_4$ (379.03): calcd. C 47.53, H 2.66, N 3.70; found C 46.60, H 2.63, N 3.59.

12b: To a mixture of 0.206 g (0.92 mmol) of $Na[NCMn(CO)_2Cp]$ and 0.308 g (0.92 mmol) of $[Cp(CO)_2Fe{\bullet}THF]BF_4$ was added 15 ml of CH_2Cl_2.The solution was stirred for 2 h and then chromatographed on a 5x1.5 cm silica-gel column using CH_2Cl_2 as eluent. A single red band moved and was collected. The solvent was removed under reduced pressure. The red residue was redissolved in 8 ml of CH_2Cl_2 and layered with 35 ml of hexane. The mixture was kept at −27°C for two days. The microcrystalline precipitate was filtered off, washed with 5 ml of hexane for 2 times and dried in vacuo. Yield 0.25 g (71%) of **12b**, red, microcrystalline, m.p.: 124°C (dec.). – IR [cm^{-1}]: $\tilde{\nu}$ = 2094m (CN), 2063s, 2018s, 1922s, 1854s (CO). – ^1H NMR: δ = 5.08 (s, 5H), 4.40 (s, 5H). – $C_{15}H_{10}NFeMnO_4$ (379.03): calcd. C 47.53, H 2.66, N 3.70; found C 46.64, H 2.65, N 3.75.

13: To a mixture of 0.072 g (0.35 mmol) of $CpFe(CO)_2CN$ and 0.208 g (0.35 mmol) of CpFe(dppe)Br was added 25 ml of CH_3OH and the solution stirred at room temperature for 0.5 h. Then to the red resulting solution was added 0.060 g (0.37 mmol) of NH_4PF_6. The resulting solution was stirred for 0.5 h. The solvent was removed under reduced pressure. The residue was extracted with 4 ml of CH_2Cl_2, and then filtered. The filtrate was layered with 15 ml of 2-propanol. The mixture was left at room temperature. After 5 h, dark-red crystals were formed which were filtered off, washed with 5 ml of hexane for 2 times and then dried in vacuo. Yield 0.176 g (60%) of **13** as dark-red crystals, m.p.: 180°C (dec.). – IR [cm^{-1}]: $\tilde{\nu}$ = 2141vw (CN), 2065s, 2026s (CO). – ^1H NMR: δ = 7.8–8.2 (m, 20 H, Ph), 4.83 (s, 5 H, Cp), 4.38 (s, 5 H, Cp), 2.75–2.80 (m, 4 H, C_2H_4). – $C_{39}H_{34}NF_6Fe_2O_2P_3$ (867.31): calcd. C 54.01, H 3.95, N 1.62; found C 53.44, H 3.91, N 1.70.

14: To a mixture of 0.124 g (0.21 mmol) of Cp(dppe)FeBr and 0.056 g (0.23 mmol) of $K[CpFe(CO)(CN)_2]$ was added 15 ml of CH_3OH and the mixture stirred for 2 h at 50°C. The solvent of the resulting red solution was removed under reduced pressure. The residue was extracted with 10 ml of benzene. By diffusion of pentane into the benzene solution red crystals were formed, which were filtered off, washed with 5 ml of hexane for 2 times and dried in vacuo. Yield 0.080 g (54%) of **14** as red crystals, m.p.: 130–133°C. – IR [cm^{-1}]: $\tilde{\nu}$ = 2118w, 2091w (CN), 1963s (CO). – ^1H NMR: δ = 7.0–8.0 (m, 20 H, Ph), 4.17 (s, 5 H, Cp), 4.08 (s, 5 H, Cp), 2.45–2.50 (m, 4 H, C_2H_4). – $C_{39}H_{34}N_2Fe_2OP_2$ (720.35): calcd. C 65.03, H 4.76, N 3.89; found C 66.32, H 5.28, N 3.45.

15a: A solution of 0.052 g (0.25 mmol) of $CpMn(CO)_3$ in 20 ml of THF was UV-irradiated for 3 h. Then to the resulting red solution containing $CpMn(CO)_2(THF)$ was added a solution of 0.136 g (0.25 mmol) of CpFe(dppe)CN in 4 ml of CH_2Cl_2. The resulting solution was stirred for 10 min and then the solvent was removed under reduced pressure. The residue was chromatographed on a 5 × 1.5 cm silica-gel column using CH_2Cl_2 as eluent. A single orange-red band moved and was collected. The collected orange-red solution was concentrated to 2 ml and then layered with 15 ml of hexane. The mixture was kept at −20°C. The crystals were filtered off, washed with 5 ml of hexane for 2 times and dried in vacuo. This yielded 0.032 g (16%) of **15a** as orange-red crystals, m.p.: 170°C (dec.). – IR [cm^{-1}]: $\tilde{\nu}$ = 2105w (CN), 1910s, 1830s (CO). – ^1H NMR: δ = 7.0–7.8 (m, 20 H, Ph), 4.18 (s, 5 H,Cp), 4.00 (s, 5 H, Cp), 2.45–2.50 (m, 4 H, C_2H_4). – $C_{40}H_{36}NCl_2FeMnP_2O_2$ (806.37): calcd. C 59.58, H 4.50, N 1.74; found C 58.64, H 4.47, N 1.75.

15b: To a mixture of 0.054 g (0.24 mmol) of $Na[NCMn(CO)_2Cp]$ and 0.145 g (0.24 mmol) of Cp(dppe)FeBr was added 8 ml of CH_3OH and the mixture stirred until all CpFe(dppe)Br was dissolved (approx. 2 h). Then the solvent was removed under reduced pressure to leave a red residue. This was chromatographed on a 5 × 1.5 cm silica-gel column using CH_2Cl_2 as eluent. A single red band moved and was collected. The solvent was removed under reduced pressure. The residue was redissolved in 4 ml of CH_2Cl_2 and layered with 15 ml of hexane. The mixture was kept at room temperature for one day. The crystals were filtered off, washed with 5 ml of hexane for 2 times and dried in vacuo. Yield 0.108 g (56%) of **15b** as red crystals, m.p.: 150°C (dec.). – IR [cm^{-1}]: $\tilde{\nu}$ = 2087m (CN), 1916s, 1845s (CO). – ^1H NMR: δ = 7.0–8.0 (m, 20 H, Ph), 4.13 (s, 5 H, Cp), 3.92 (s, 5 H, Cp), 2.45–2.50 (m, 4 H, C_2H_4). – $C_{40}H_{36}NCl_2FeMnP_2O_2$ (806.37): calcd. C 59.58, H 4.50, N 1.74; found C 59.29, H 4.43, N 1.72.

16: To a mixture of 0.120 g (0.20 mmol) of Cp(dppe)FeBr and 0.142 g (0.20 mmol) of $Cp(PPh_3)_2RuCN$ was added 20 ml of

CH_3OH and the mixture stirred overnight. To the resulting red solution 0.064 g (0.40 mmol) of solid NH_4PF_6 was added and the solution stirred further for 1 h. This led to the precipitation of the product and left a pale orange solution. The precipitate was filtered off and dried in vacuo. It was dissolved in 6 ml of CH_2Cl_2 and then filtered to give a red filtrate. The red filtrate was layered with 30 ml of 2-propanol and the mixture left at room temperature for 2 d. This yielded 0.21 g (69%) of **16** as red microcrystalline material, m.p. 208°C (dec.). – IR [cm^{-1}]: $\tilde{\nu}$ = 2069w (CN). – ^1H NMR: δ = 7.0–8.1 (m, 50 H, Ph), 4.32 (s, 5 H, Cp), 3.88 (s, 5 H, Cp), 2.45–2.55 (m, 4 H, C_2H_4). – $C_{74}H_{66}Cl_2NF_6FeP_5Ru$ (1466.1): calcd. C 60.57, H 4.50, N 0.95; found C 61.42, H 4.56, N 0.92.

Oxidations

2a-ox: To a solution of 0.054 g (0.073 mmol)of **2a** in 6 ml of CH_2Cl_2 was added 0.042 g (0.073 mmol) of $[(BrC_6H_4)_3N]BF_4$ and the solution stirred for 10 min. The solvent of the resulting dark brown solution was removed under reduced pressure and the residue was washed four times with 6 ml of diethyl ether. Then the residue was redissolved in 5 ml of CH_2Cl_2 and layered with 10 ml of Et_2O. The mixture was kept at room temperature overnight. After filtration, washing with 5 ml of diethyl ether for 2 times and drying in vacuo, 0.052 g (87%) of **2a-ox** as dark-brown crystals, m.p.: 108°C (dec.), were obtained. – IR [cm^{-1}]: $\tilde{\nu}$ = 2011m (CN), 2077w, 1949s (CO). – $C_{37}H_{29}NBCrF_4FeO_5P_2$ (824.24): calcd. C 53.92, H 3.55, N 1.70; found C 53.63, H 3.50, N 1.65.

6-ox: The same procedure as for **2a-ox** was used except using 0.043 g (0.055 mmol) of **6** and 0.030 g (0.053 mmol) of $[(BrC_6H_4)_3N]BF_4$. Yield 0.013 g (28%) of **6-ox** as brown crystals, m.p.: 130°C (dec.). – IR [cm^{-1}]: $\tilde{\nu}$ = 2021m (CN), 2091w, 1991w, 1935s (CO). – $C_{37}H_{29}NBF_4FeMoO_5P_2$ (868.18): calcd. C 51.19, H 3.37, N 1.61; found C 50.79, H 3.27, N 1.57.

8-ox: The same procedure as for **2a-ox** was used except using 0.044 g (0.051 mmol) of **8** and 0.030 g (0.053 mmol) of $[(BrC_6H_4)_3N]BF_4$. Yield 0.015 g (31%) of **8-ox** as dark brown crystals, m.p. 158°C (dec.). – IR [cm^{-1}]: $\tilde{\nu}$ = 2016m (CN), 2091w, 1986w, 1926s (CO). – $C_{37}H_{29}NBF_4FeO_5P_2W$ (956.09): calcd. C 46.48, H 3.06, N 1.47; found C 45.77, H 3.00, N 1.46.

13-ox: To a mixture of 0.045 g (0.054 mmol) of **13** and 0.018 g (0.054 mmol) of $[Cp_2Fe]PF_6$ was added 5 ml of CH_2Cl_2 forming a dark red solution. The solution was layered with 6 ml of diethyl ether. After 2 h filtration, washing with 5 ml of diethyl ether for 2 times and drying in vacuo yielded 0.050 g (91%) of **13-ox** as dark-red microcrystals, m.p.: 174°C (dec.). – IR [cm^{-1}]: $\tilde{\nu}$ = 2116s (CN), 2065s, 2030s (CO). – $C_{39}H_{34}NF_{12}Fe_2O_2P_4$ (1012.27): calcd. C 46.27, H 3.39, N 1.38; found C 45.58, H 3.32, N 1.32.

14-ox: To a mixture of 72 mg (0.10 mmol) of **14** and 34 mg (0.10 mmol) of $[Cp_2Fe](PF_6)$ was added 6 ml of CH_2Cl_2 and the solution stirred for 0.5 h. A green solution was formed. The reaction solution was filtered and the filtrate layered with 10 ml of diethyl ether. The mixture was kept at −20°C for one day. After filtration, washing with 5 ml of diethyl ether for 2 times and drying in vacuo, 75 mg (86%) of **14-ox** as dark-green microcrystals were obtained, m.p.: 246°C (dec.). – IR [cm^{-1}]: $\tilde{\nu}$ = 2099w, 2056s (CN), 1982s (CO). – $C_{40}H_{36}Cl_2N_2F_{12}Fe_2OP_4$ (950.25): calcd. C 50.56, H 3.82, N 2.95; found C 51.59, H 3.72, N 3.10.

16-ox: To a solution of 138 mg (0.10 mmol) of **16** in 15 ml of CH_2Cl_2 was added 33 mg (0.10 mmol) of $[Cp_2Fe](PF_6)$ and the solution stirred for 15 min. A dark-green solution was obtained. After filtration, the filtrate was layered with 15 ml of diethyl ether and the mixture kept at room temperature overnight. After filtration, washing with 5 ml of diethyl ether for 2 times and drying in vacuo, 120 mg (79%) of **16-ox** as dark-green crystals were obtained, m.p. 172°C (dec.). – IR [cm^{-1}]: $\tilde{\nu}$ = 1996m (CN). – $C_{74}H_{66}Cl_2NF_{12}FeP_6Ru$ (1611.1): calcd. C 55.12, H 4.10, N 0.87; found C 54.65, H 4.24, N 0.97.

Structure Determinations[60]: Crystals of **2a** and **2b** were obtained from dichloromethane/hexane, those of **3** from benzene/hexane and

Table 10. Crystallographic details

	2a	**2b**	**2a-ox**	**3**	**4**
formula	$C_{27}H_{29}CrFeNO_5P_2$	$C_{37}H_{29}CrFeNO_5P_2$	$C_{37}H_{29}BCrF_4FeNO_5P_2$	$C_{29}H_{20}CrNNiO_5P$	$C_{42}H_{30}AgCrNO_5P_2$
mol. mass	737.40	737.40	824.21	604.14	850.48
color	red	yellow	dark brown	brown	colorless
crystal size [mm]	0.7 × 0.4 × 0.3	0.7 × 0.4 × 0.4	0.5 × 0.3 × 0.15	0.8 × 0.4 × 0.4	0.5 × 0.4 × 0.2
space group	$P2_1/c$	$P2_1/c$	$P2_1/c$	$P-1$	$C2/c$
Z	4	4	4	4	4
a [Å]	15.014(1)	15.007(1)	18.290(4)	11.481(2)	12.990(3)
b [Å]	12.995(1)	12.976(1)	11.109(2)	12.267(2)	23.134(3)
c [Å]	17.182(1)	17.164(2)	19.153(4)	20.947(4)	14.274(3)
α [°]	90	90	90	82.58(3)	90
β [°]	95.49(1)	95.60(1)	107.55(3)	76.47(3)	106.36(3)
γ [°]	90	90	90	78.98(3)	90
V [Å^3]	3336.9(4)	3326.4(5)	3710(1)	2804(1)	4116(2)
$d_{calcd.}$[g/cm^3]	1.47	1.47	1.48	1.43	1.37
μ [mm^{-1}]	0.90	0.90	0.83	1.15	0.86
2Θ range	4.5–52	4.5–52	4.5–50	4.5–52.5	5 to 52.5
hkl ranges	*h*: −18 to 18 *k*: −16 to 0 *l*: −21 to 0	*h*: −18 to 18 *k*: −15 to 0 *l*: −21 to 0	*h*: −21 to 0 *k*: −13 to 0 *l*: −21 to 22	*h*: −14 to 0 *k*: −15 to 15 *l*: −26 to 25	*h*: −16 to 15 *k*: 0 to 28 *l*: 0 to 17
refl. measd.	6773	6742	6728	13133	4360
indep. refl.	6543	6512	6512	11369	4187
obsd. refl. [$I \geq 2\sigma(I)$]	5034	5314	2677	8053	1990
parameters	424	424	292	685	238
$R1$ (obsd. refl.)	0.068	0.045	0.078	0.039	0.069
$wR2$(all refl.)	0.229	0.173	0.254	0.119	0.219
res. el. density [e/Å^3]	+1.2, −1.7	+0.7, −0.7	+0.8, −0.5	+0.5, −0.4	+0.9, −0.8

of **4** from dichloromethane/ethanol, those of **2a-ox** from dichloromethane/diethyl ether. Diffraction data were recorded at room temperature with the ω/2&thetas; technique on a Nonius CAD4 diffractometer fitted with a molybdenum tube (K_α, $\lambda = 0.7107$ Å) and a graphite monochromator. Semiempirical absorption corrections based on ψ scans were applied. The structures were solved with direct methods and refined anisotropically with the SHELX program suite.[61] Hydrogen atoms were included with fixed distances and isotropic temperature factors 1.2 times those of their attached atoms. Parameters were refined against F^2. The R values are defined as $R_1 = \Sigma|F_o - F_c|/\Sigma F_o$ and $wR_2 = [\Sigma[w(F_o^2 - F_c^2)^2/\Sigma[w(F_o^2)^2]]]^{1/2}$. Drawings were produced with SCHAKAL.[62] Table 10 lists the crystallographic data.

[1] T. Mallah, S. Thiebaut, M. Verdaguer, P. Veillet, *Science* **1993**, *262*, 1554–1557.
[2] W. R. Entley, G. Girolami, *Science* **1995**, *268*, 397–402.
[3] O. Sato, T. Iyoda, A. Fujishima, K. Hashimoto, *Science* **1996**, *271*, 49–51.
[4] D. W. Knoeppel, S. G. Shore, *Inorg. Chem.* **1996**, *35*, 1747–1748.
[5] J. Lu, W. T. A. Harrison, A. J. Jacobson, *J. Chem. Soc., Chem. Commun.* **1996**, 399–400.
[6] H. Miyasaka, N. Matsumoto, H. Okawa, N. Re, E. Gallo, C. Floriani, *J. Am. Chem. Soc.* **1996**, *118*, 981–994.
[7] M. Ohba, H. Okawa, T. Ito, A. Ohto, *J. Chem. Soc., Chem. Commun.* **1995**, 1545–1546.
[8] J. Metz, M. Hanack, *J. Am. Chem. Soc.* **1983**, *105*, 828–830.
[9] C. A. Bignozzi, R. Argazzi, C. G. Garcia, F. Scandola, J. R. Schoonover, T. J. Meyer, *J. Am. Chem. Soc.* **1992**, *114*, 8727–8729.
[10] F. L. Atkinson, N. C. Brown, N. G. Connelly, A. G. Orpen, A. L. Rieger, P. H. Rieger, G. M. Rosair, *J. Chem. Soc., Dalton Trans.* **1996**, 1959–1966.
[11] G. A. Carriedo, N. G. Connelly, M. C. Crespo, I. C. Quarmby, V. Riera, G. H. Worth, *J. Chem. Soc., Dalton Trans.* **1991**, 315–323.
[12] W. P. Fehlhammer, M. Fritz, *Chem. Rev.* **1993**, *93*, 1243–1280.
[13] V. O. Kennedy, C. L. Stern, D. F. Shriver, *Inorg. Chem.* **1994**, *33*, 5967–5969.
[14] C. A. Bignozzi, R. Argazzi, C. Chiorboli, S. Roffia, F. Scandola, *Coord. Chem. Rev.* **1991**, *111*, 261–266.
[15] F. Scandola, R. Argazzi, C. A. Bignozzi, C. Chiorboli, M. T. Indelli, M. A. Rampi, *Coord. Chem. Rev.* 1993, *125*, 283–292.
[16] A. Burewicz, A. Haim, *Inorg. Chem.* **1988**, *27*, 1611–1614.
[17] H. Kunkely, V. Pawlowski, A. Vogler, *Inorg. Chim. Acta* **1994**, *225*, 327–330.
[18] W. M. Laidlaw, R. G. Denning, *J. Chem. Soc., Dalton Trans.* **1994**, 1987–1994. W. M. Laidlaw, R. G. Denning, *Inorg. Chim. Acta* **1996** *248*, 51–58.
[19] D. F. Shriver, *Struct. Bonding (Berlin)* **1966**, *1*, 32–58.
[20] M. J. Scott, S. C. Lee, R. H. Holm, *Inorg. Chem.* **1994**, *33*, 4651–4662.
[21] D. J. Darensbourg, J. C. Yoder, M. W. Holtcamp, K. K. Klausmeyer, J. H. Reibenspies, *Inorg. Chem.* **1996**, *35*, 4764–4769.
[22] H. Vahrenkamp, *Pure Appl. Chem.* **1991**, *63*, 643–649. H. Vahrenkamp in *Organometallics in Organic Synthesis*, vol. 2 (Eds.: H. Werner, G. Erker), Springer, Berlin, **1989**, pp 235–254.
[23] B. Oswald, A. K. Powell, F. Rashwan, J. Heinze, H. Vahrenkamp, *Chem. Ber.* **1990**, *123*, 243–250.
[24] N. Zhu, P. Hauser, J. Heinze, H. Vahrenkamp, *J. Cluster Sci.* **1995**, *6*, 147–162.
[25] N. Zhu, J. Pebler, H. Vahrenkamp, *Angew. Chem.* **1996**, *108*, 984–985; *Angew. Chem. Int. Ed. Engl.* **1996**, *35*, 894–895.
[26] H. Vahrenkamp in *The Synergy Between Dynamics and Reactivity at Clusters and Surfaces* (Ed.: L. J. Farrugia), Kluwer, Dordrecht, **1995**, pp 297–316.
[27] N. Zhu, H. Vahrenkamp, *J. Organomet. Chem.* **1994**, *472*, C5–C7.
[28] N. Zhu, H. Vahrenkamp, *Angew. Chem.* **1994**, *106*, 2166–2167; *Angew. Chem. Int. Ed. Engl.* **1994**, *33*, 2090–2091.
[29] H. Behrens, J. Kohler, *Z. Anorg. Allg. Chem.* **1960**, *306*, 94–101.
[30] J. K. Ruff, *Inorg. Chem.* **1969**, *8*, 86–89.
[31] G. J. Baird, S. G. Davies, S. D. Moon, S. J. Simpson, *J. Chem. Soc., Dalton Trans.* **1985**, 1479–1486.
[32] F. R. Fronczek, W. P. Schaefer, *Inorg. Chem.* **1974**, *13*, 727–732.
[33] D. Gaswick, A. Haim, *J. Inorg. Nucl. Chem.* **1978**, *40*, 437–439.
[34] A. G. Sharpe, *The Chemistry of Cyano Complexes of the Transition Metals*, Academic Press, New York, **1976**.
[35] A. M. Golub, H. Köhler, V. V. Skopenko in *Chemistry of Pseudohalides* (Ed.: R. J. H. Clark), Elsevier, Amsterdam, **1986**, pp. 77–185.
[36] M. R. Churchill, T. A. O'Brien, *J. Chem. Soc. A* **1970**, 161–167, and references cited therein.
[37] J. Darkwa, F. Bothata, L. M. Koczon, *J. Organomet. Chem.* **1993**, *455*, 235–240.
[38] G. Wulfsberg, D. Jackson, W. Ilsley, S. Q. Dou, A. Weis, *Z. Naturforsch., A: Phys. Sci.* **1992**, *47*, 75–84.
[39] F. A. Cotton, C. S. Kraihanzel, *J. Am. Chem. Soc.* **1962**, *84*, 4432–4438. F. A. Cotton, *Inorg. Chem.* **1964**, *3*, 702–711.
[40] S. Alvarez, C. Lopez, M. J. Bermejo, *Trans. Met. Chem. (London)* **1984**, *9*, 123–126, and references cited therein.
[41] G. A. Carriedo, N. G. Counelly, S. Alvarez, E. Perez-Carreño, S. Garcia-Grande, *Inorg. Chem.* **1993**, *32*, 272–276.
[42] M. B. Robin, P. Day, *Adv. Inorg. Chem. Radiochem.* **1967**, *10*, 247–422.
[43] N. S. Hush, *Prog. Inorg. Chem.* **1967**, *8*, 391–444.
[44] J. C. Curtis, B. P. Sullivan, T. J. Meyer, *Inorg. Chem.* **1983**, *22*, 224–236.
[45] V. Gutmann, *Electrochim. Acta* **1976**, *21*, 661–670.
[46] Y. Marcus, *Chem. Soc. Rev.* **1993**, *22*, 409–416.
[47] A. Martinsen, J. Songstad, *Acta. Chem. Scand., Ser. A* **1977**, *A31*, 645–650.
[48] W. Strohmeier, K. Gerlach, *Chem. Ber.* **1961**, *94*, 398–406.
[49] E. O. Fischer, R. J. Schneider, *J. Organomet. Chem.* **1968**, *12*, P27–P30.
[50] R. B. King, *Inorg. Chem.* **1967**, *6*, 25–29.
[51] W. P. Fehlhammer, W. A. Herrmann, K. Öfele, in G. Brauer, *Handbuch der Präparativen Anorganischen Chemie*, 3rd. ed., Enke Verlag, Stuttgart, **1981**, vol. 3, p. 1999–2000.
[52] C. E. Coffey, *J. Inorg. Nucl. Chem.* **1963**, *25*, 179–185.
[53] B. D. Dombek, R. J. Angelici, *Inorg. Chim. Acta* **1973**, *7*, 345–347.
[54] G. J. Baird, S. G. Davies, *J. Organomet. Chem.* **1984**, *262*, 215–221.
[55] S. Du, N. Zhu, P. Chen, X. Wu, J. Lu, *J. Chem. Soc., Dalton Trans.* **1992**, 339–344.
[56] K. W. Barnett, *J. Chem. Educ.* **1974**, *51*, 422–423.
[57] D. L. Reger, C. Coleman, *J. Organomet. Chem.* **1977**, *131*, 153–162. H. Schumann, *J. Organomet. Chem.* **1986**, *304*, 341–351.
[58] R. B. King, L. W. Houk, K. H. Pannell, *Inorg. Chem.* **1969**, *8*, 1042–1048.
[59] M. I. Bruce, C. Hameister, A. G. Swincer, R. C. Wallis, *Inorg. Synth.* **1980**, *21*, 78–80.
[60] Crystallographic data (excluding structure factors) for the structures reported in this paper have been deposited with the Cambridge Crystallographic Data Centre as supplementary publication no. CCDC-100389. Copies of the data can be obtained free of charge on application to The Director, CCDC,12 Union Road, Cambridge CB2 1EZ, UK [fax: int. code +44(1223)336-033, e-mail: deposit@chemcrys.cam.ac. uk].
[61] G. M. Sheldrick, *SHELX-86* and *SHELXL-93* (Programs for Crystal Structure Determination), Universität Göttingen, **1986** and **1993**.
[62] E. Keller, *SCHAKAL*, Universität Freiburg, **1993**.

[97101]